Differential sensitivity to temperature and evaporative demand in wheat relatives

Stéphane Leveau, Boris Parent, Serge Zaka, Pierre Martre

Journal of Experimental Botany, Vol. 72, No. 21 pp. 7580–7593, 2021
https://doi.org/10.1093/jxb/erab431 Advance Access Publication 24 September 2021
This paper is available online free of all access charges (see https://academic.oup.com/jxb/pages/openaccess for further details)

RESEARCH PAPER

Differential sensitivity to temperature and evaporative demand in wheat relatives

Stéphane Leveau[1,2], Boris Parent[1,*], Serge Zaka[2] and Pierre Martre[1,*]

[1] LEPSE, Université de Montpellier, INRAE, Institut Agro, Montpellier, France
[2] ITK, Clapiers, France

* Correspondence: boris.parent@inrae.fr or pierre.martre@inrae.fr

Received 12 July 2021; Editorial decision 23 August 2021; Accepted 23 September 2021

Editor: Greg Rebetzke, CSIRO Agriculture and Food, Australia

Abstract

There are potential sources of alleles and genes currently present in wheat-related species that have the potential to be introduced into wheat breeding programs targeting current and future hot and dry climates. However, to date neither the intra- nor the interspecific diversity of the responses of leaf growth and transpiration to temperature and evaporative demand have been investigated in across a significant range of wheat-related species. By analysing 12 groups of wheat-related species and subspecies, we were able to examine the multi-dimensional structure of the genetic diversity for traits linked to plant vegetative structures and their development, and to leaf expansion and transpiration, together with their responses to 'non-stressing' ranges of temperature and evaporative demand. In addition to providing new insights on how genome type, ploidy level, phylogeny, and breeding pressure act together to structure this genetic diversity, our study also provides new mathematical formalisms and associated parameters for trait responses across a wide range of genetic diversity in wheat-related species. This will potentially allow crop models to predict the impact of this diversity on yield, and thus to indicate potential sources of varietal improvement for modern wheat germplasms through interspecific crosses.

Keywords: *Aegilops*, evaporative demand, genetic diversity, leaf expansion, leaf growth, temperature, transpiration, *Triticum*, vapour pressure deficit (VPD), wheat.

Introduction

Cereal production worldwide is affected by high temperature, high evaporative demand, and drought (Lobell *et al.*, 2011). The frequency of such events is increasing as a result of climate change (Handmer *et al.*, 2012; Ben-Ari *et al.*, 2018; Rojas *et al.*, 2019), while at the same time agriculture is being challenged by societal and policy requirements for more sustainable and water-sparing production methods. Developing new cultivars that are adapted to meet the needs of this dual context is not straightforward, given the wide range of climates and management practices in wheat-growing regions and the fact that an individual genotypic trait can have positive effects on crop performance in one type of environment while being deleterious in another (Tardieu, 2012).

A purely experimental approach cannot explore the effects on yield, plant resilience, and environmental balances of each combination of traits under all possible environmental

scenarios. A combination of experimental and modelling approaches is therefore required to define the best combination of traits in a given target environment (Reyer *et al.*, 2013; Jeuffroy *et al.*, 2014; Perego *et al.*, 2014; Rotter *et al.*, 2015), using models that predict genotypic effects under various environmental scenarios (Parent and Tardieu, 2014). These models require formalisms of specific responses to environmental constraints that are adapted to encompass large genetic variability, together with associated trait/parameter values that also cover the wide range of variability that breeders can encounter within enlarged breeding pools (Hammer *et al.*, 2019). This has not yet been achieved for the responses of leaf expansion and transpiration to temperature and evaporative demand in crop growth models for wheat. This is despite the fact that, for example, the control of transpiration under high evaporative demand can be a key factor in designing future cultivars that can produce 'more crop per drop' (Davies *et al.*, 2001). In wheat models, the availability of efficient formalisms and parameter values differ greatly between processes, as follows.

The response of leaf expansion to temperature has been found to be similar to that of plant development (Parent *et al.*, 2019), at least within a 'non-stressing' range in which processes are not durably affected, and are reversible (Parent *et al.*, 2010). Within such ranges, which are not considered as 'heat' or 'cold' stresses, development responses to temperature are well-formalized and parameter values have been determined in most cultivated species. Indeed, these responses are the basis of the calculation of thermal time, a central concept of most process-based models. Parent and Tardieu, (2012) reported a very low variability of this response within each species they studied, while a wider variability was present between species. However, to date, the variability of temperature responses—and the possibility of seeking new alleles controlling these responses—between closely-related species such as within different wheats has not been documented.

While evaporative demand has been found as mostly affecting leaf expansion rate in several species (e.g. Parent *et al.*, 2010; Tardieu *et al.*, 2014), very little is known about how growth is affected in wheat and whether significant genetic variability exists in it and related species. This is probably due to the fact that temperature and vapour-pressure deficit (VPD) are difficult to dissociate in natural environments. There is an urgent need to characterize these responses, both for the accuracy of model predictions and to inform wheat breeders on the availability (or not) of associated genetic variability.

The response of transpiration to VPD has been studied in several crops including wheat (Schoppach and Sadok, 2012; Schoppach *et al.*, 2017). In wheat, breeders have indirectly selected genotypes that present a limitation in hydraulic conductance (Schoppach *et al.*, 2017), allowing decreased transpiration at high VPD. However, we do not know if the reported range of responses represents most of the total genetic variability in wheat-related species, or if some genetic variability has been lost during wheat domestication and breeding.

Wheat-related species form a large family (>300 species and subspecies), including wild and cultivated species domesticated over 10 000 years, three subgenomes (A, B, and D), and three levels of ploidy (diploids: A^u, A^m, B, and D genome; tetraploids: AB subgenomes; hexaploids: ABD subgenomes). Polyploid *Triticum* species originated by natural hybridization events between *Triticum* and *Aegilops* species (Fig. 1) (Petersen *et al.*, 2006). Bread wheat (*T. aestivum*) represents 95% of global wheat production and is grown across very wide ranges of latitude and altitude (Curtis *et al.*, 2002). Durum wheat (*T. turgidum* subsp. *durum*) is mainly grown under Mediterranean-type climates. Other wheat species are grown more marginally, such as spelt (*T. aestivum* subsp. *spelta*), einkorn (*T. monococcum* subsp. *monococcum*), and emmer wheat (*T. turgidum* subsp. *dicoccum*).

Because of the availability of wild wheat-related species, there is a large reservoir of alleles and genes that can potentially be introduced into wheat breeding programs through interspecific crosses. For example, bread wheat emerged from the natural hybridization between wild goatgrass (*Ae. tauschii*) and a tetraploid wheat (*T. turgidum* subsp. *dicocccum*, a progenitor of modern durum wheat). However, the genetic diversities of *T. turgidum* and *Ae. tauschii* are not fully represented in *T. aestivum*, probably because it has evolved from only a few hybridization events. Introducing genes from wheat-relative species can therefore increase the genetic diversity of modern germplasms (Gorafi *et al.*, 2018), for example as seen in synthetic crosses between tetraploid wheats and *Ae. tauschii* (Rosyara *et al.*, 2019) and between *T. aestivum and T. turgidum* (Martin *et al.*, 2011).

The higher tolerance of durum wheat to heat and drought stress compared with bread wheat is still debated (Marti and Slafer, 2014; Giunta *et al.*, 2019), and comparisons have generally been performed based only on yield or yield components, and our knowledge regarding the differences in plant responses to abiotic constraints is still limited (Allahverdiyev, 2015). Physiological responses at fine scales can be very different from macroscopic responses, which emerge as properties of numerous underlying processes, integrated over the whole growth cycle (Tardieu and Parent, 2017).

Such interspecific genetic variability can originate not only from genes or alleles currently residing in wild species but also from ploidy itself. Traits expressed in wild diploids might not predict the traits in progeny of higher ploidy after synthetic hybridizations. Indeed, ploidy itself can provide agronomic advantages or disadvantages (Comai, 2005), for example by conferring resistance to biotic and abiotic stresses (Tu *et al.*, 2014; Schoenfelder and Fox, 2015; Hias *et al.*, 2018).

In this study, we analysed 12 groups of wheat-related species and subspecies (five accessions each) for traits linked to vegetative structure and development, and to leaf expansion and transpiration, together with their responses to ranges of 'non-stressing' temperatures and evaporative demand during the

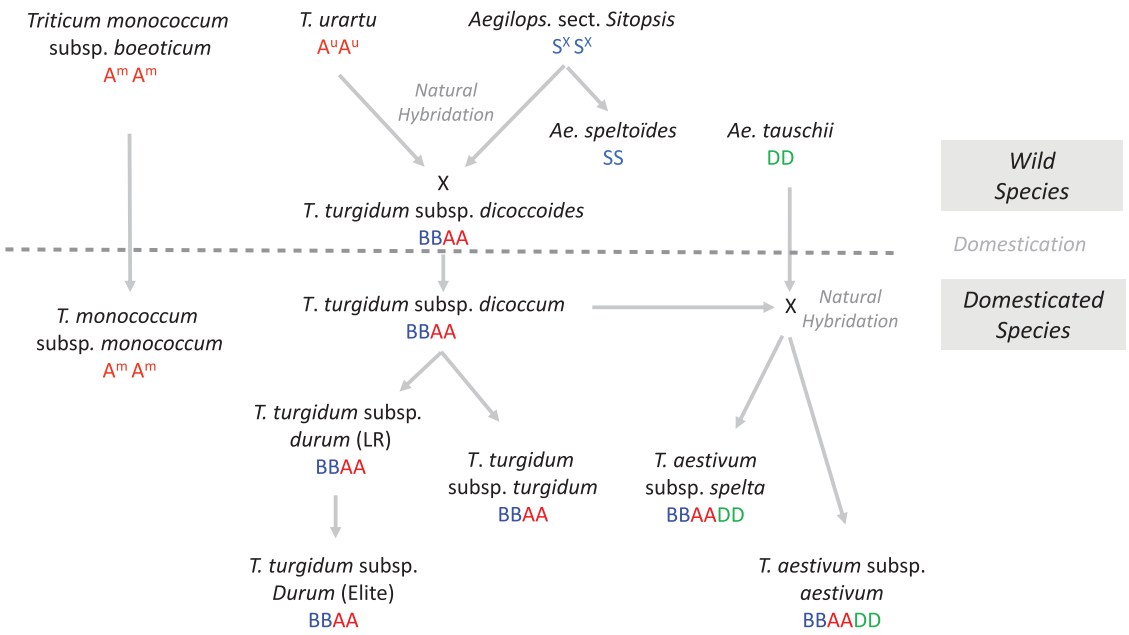

Fig. 1. The evolutionary and genome relationships between the cultivated wheat species and related wild species used in this study. The origin of the B genome is still unclear but it comes from a species of *Ae.* sect. *Sitopsis*, represented here by *Ae. speltoides*. *Triticum turgidum* subsp. *durum* was separated in two groups: landrace populations (LR) grown before the Green Revolution and elite cultivars released afterwards.

vegetative phase. We used an original experimental protocol and selected model formalisms adapted to this broad genetic diversity in order to compare the intra- and interspecific diversities. We determined that the genome type, ploidy level, and phylogeny act together to structure the genetic diversity, and that breeding pressure may have indirectly pushed these traits in specific directions. Overall, in addition to providing new formalisms of trait responses together with model parameters to be included in process-based models for large-scale simulations, this study indicates potential sources of varietal improvement for modern wheat germplasms that currently reside in related species.

Materials and methods

Plant material

We analysed 12 wheat-related species and subspecies (Fig. 1) and selected five accessions per species in order to maximize the genetic diversity within each (Supplementary Tables S1, S2). This set included wild and cultivated species with different levels of ploidy, as follows.

Wild diploid species: *Triticum monococcum* subsp. *boeticumm* (A^m genome), *T. urartu* (A^u genome), *Aegilops tauschii* (D genome), and *Ae. speltoides* (S genome, related to species belonging to *Ae.* sect. *sitopsis* from which the B genome originated).

Cultivated diploid species: einkorn wheat *T. monococcum* subsp. *monococcum* (A^m genome), domesticated from *T. monococcum* subsp. *Boeticumm*.

Wild tetraploid species: wild emmer wheat *T. turgidum* subsp. *dicoccoides* (AB genome), originating from a natural hybridization event between *T. uratu* and an unknown species belonging to *Aegilops* sect. *sitopsis*.

Cultivated tetraploid species: cultivated emmer wheat *T. turgidum* subsp. *dicoccum* (AB genome), domesticated from wild emmer wheat, rivet wheat (or poulard wheat, *T. turgidum* subsp. *turgidum*; AB genome), which evolved from *T. turgidum* subsp. *dicoccum*, and durum wheat (*T. turgidum* subsp. *durum*; AB genome), which was domesticated from *T. turgidum* subsp. *dicoccum*. We separated these into two groups: landraces from before and elite cultivars released after the 'Green Revolution'.

Cultivated hexaploid wheats: spelt wheat (*T. aestivum* subsp. *spelta*, ABD genome) and bread wheat (*T. aestivum* subsp. *aestivum*, ABD genome) originating from natural hybridization events between *T. turgidum* subsp. *dicoccum* and *Ae. tauschii*.

Plant growth conditions

All experiments were conducted in the plant phenotyping platform Phenodyn, part of the plant phenotyping platforms of M3P (Montpellier, France, https://www6.montpellier.inrae.fr/lepse_eng/M3P). Briefly, this platform is set up with balances to monitor plant transpiration, displacement transducers to monitor leaf expansion, a set of climatic sensors, and automatic drip-feed systems. Air temperature, relative humidity, and photosynthetic photon flux density (PPFD) at the plant level were measured and stored every 15 min in a datalogger (CR10X, Campbell Scientific Ltd, Leicestershire, UK). The temperature of the leaf meristematic (growth) zone was measured using thermocouples inserted vertically inside the sheath of leaf 5 of 3–6 plants, and used to calculate meristem-to-air VPD. VPD was controlled based on measurements of relative humidity and temperature.

Seeds were imbibed for 24 h at 4 °C on water-saturated filter papers in Petri dishes, then placed at room temperature for 24 h before being returned to 4 °C for 48 h. Six germinated seeds each were planted in 9-l plastic pots (20 cm diameter) filled with a 40:60 (v:v) mixture of clay and organic compost, and then thinned to three uniform plants per pot when the third leaf emerged. A total of three pots (nine plants) per accession were used, together with four pots containing non-transpiring artificial plastic plants mimicking real ones that were used to calculate evaporation from the soil surface. Sowing was spread over 11 weeks in order to stagger measurements in the growth chambers. A fully randomized design was used. Pots with fewer than three emerged plants were replaced with newly sown ones during the 12th week.

Plants were grown for the first 3 weeks in a growth chamber where temperature and VPD were controlled at 20.6±2.6 /16.3±1.9 °C and 1.4±0.4/0.9±0.3 kPa (day/night), respectively. PPFD at plant level averaged 300 µmol s^{-1} m^{-2} during the 12-h photoperiod. Plants were watered daily to maintain the soil water potential above –0.05 MPa. At 3 weeks after plant emergence, two pots (six plants) of each accession were transferred to another growth chamber and were subjected to varying temperature and VPD conditions (scenario 1) over a 4-d period, whilst one pot (three plants) was subjected to a second scenario (scenario 2) with more extreme temperatures (Supplementary Fig. S1). This period of treatment was selected because it corresponded to the appearance of leaf 5 in all the genotypes, and it allowed the comparison of absolute values of leaf elongation rate because internode elongation had not started yet. At later plant stages, the automatic measurement of elongation with displacement transducers did not make it possible to discriminate between the elongations of internodes and leaves. For both scenarios, the plants were harvested at the end of the 4-d period. We used the two scenarios applied in different growth chambers and on different plants to compare the response of leaf elongation rate (LER) to temperature on plants at similar development stages over the full range of target temperatures.

In scenario 1, each night the plants were subjected to two air temperatures: a reference temperature of 20 °C for 6 h, and a target temperature of either 12, 16, 24, or 28 °C for the other 6 h. The lowest temperature between the reference and the target was applied first. For the first 3 d, during the light period the plants were subjected to two VPD values: a 6-h period with a reference VPD of 1.3 kPa and a 6-h period with a target VPD value of either 0.5, 2.5, or 3.0 kPa. Again, the lowest VPD value was applied first. The daytime air temperature was set in such a way that the target air VPD values were attainable (20 °C for 0.5 kPa, 26 °C at 2.5 kPa, and 28 °C at 3.0 kPa), but in all cases the temperature was similar for both the reference and the tested VPD. On the fourth day, the air temperature and VPD were maintained at 20 °C and 1.3 kPa, respectively.

In scenario 2, a protocol similar to that of scenario 1 was applied but with more extreme temperatures and VPD values. The target night-time air temperatures were 4, 8, 32, and 36 °C, and the target day-time VPD values were 0.3, 2.5, and 4 kPa. However, we found that VPD was not sufficiently stable under these conditions, and hence in later analyses we used the data for plant responses to night temperature not the data obtained during the light period. As in scenario 1, on the fourth day the temperature was maintained at 20 °C and VPD at 1.3 kPa.

Response of leaf elongation rate to temperature

The youngest growing leaf (which was leaf 4 or 5 during the first night, and leaf 5 or 6 for the last day of measurements) was attached to a rotary displacement transducer (601–1045 Full 360 Smart Position Sensor; Spectrol Electronics, Ltd, Wiltshire, UK). Leaf elongation was transmitted to the sensor via a pulley attached to it, which carried a thread attached to the leaf tip and to a 10-g counterweight. Leaf elongation was recorded on the datalogger every 15 min.

The response of LER to the temperature of the leaf growth zone was calculated from both the temperature scenarios during the night period in order to avoid confounding effects of temperature and evaporative demand. In all cases, LER stabilized within 2 h after the beginning of the night period or after the change in temperature (Fig. 2; checked on all plants). LER was therefore averaged over the last 4 h of each period. In wheat, the LER of a given leaf is not steady and depends on leaf rank. Therefore, in order to compare leaves of different lengths (relative to their final length) and rank, the LER at the target temperature was normalized by LER at the reference temperature (20 °C) measured during the same night. To determine the cardinal temperatures of normalized LER, the data were fitted with a 3-parameter segmented linear-function equation constrained to be equal to 1 at the reference temperature:

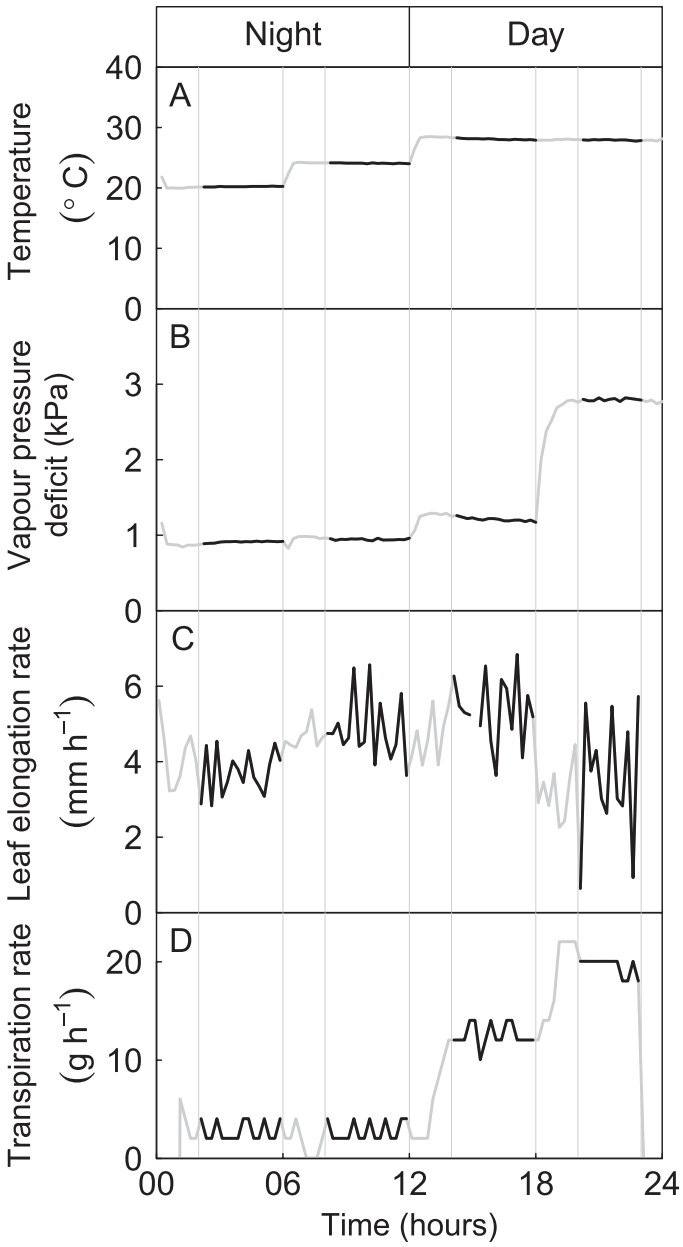

Fig. 2. Illustration of time-courses of air temperature and vapour-pressure deficit (VPD) applied to plants, and example responses. (A) Air temperature and (B) VPD regimes, (C) leaf elongation rate (LER), and (D) transpiration rate (TR). Measurements were taken during Day 3 of scenario 1 (see Supplementary Fig. S1). The vertical grey lines indicate the 4-h periods during which the environmental conditions were considered to be stable, and the mean values of LER and TR were determined during these periods (black lines). The data in (C, D) are from *T. turgidum* subsp. *durum*, cultivar Brumaire. All measurement were performed on the same plant.

$$f(T) = \begin{cases} \frac{(T-T_{\min})}{(T_{\text{ref}}-T_{\min})}, & T < T_{\text{opt}} \\ \frac{(T-T_{\max})(T_{\text{opt}}-T_{\min})}{(T_{\text{ref}}-T_{\min})(T_{\text{opt}}-T_{\max})}, & T \geq T_{\text{opt}} \end{cases} \quad (1)$$

where T is the temperature of the leaf meristematic zone, T_{ref} is the reference temperature at which $f(T)$ is equal to 1, $T_{\min}$ is the base temperature

Table 1. Summary of the phenotypic structural, rate, and response traits measured in this study

Trait type	Abbreviation	Units	Definition
Structural	LA2	cm^2	Leaf area of leaf 2
	rlw2	–	Length/width ratio for leaf 2
	TL	Leaves $plant^{-1}$	Total number of leaves per plant (main stem + tillers)
	LAT	cm^2 $plant^{-1}$	Leaf area per plant (sheath + leaf blade)
	MLA	g m^{-2}	Specific leaf mass
	r_{LA}	–	Ratio of sheath to blade leaf area
	s_{LAK}	–	Slope of the relationship between individual leaf area and leaf rank, normalized by the area of leaf 2
	PN	g N $plant^{-1}$	Shoot nitrogen mass per plant
	SLN	g N m^{-2}	Specific leaf (sheath + blade) nitrogen
Rates	LERm	mm h^{-1}	Maximal elongation rate of leaf 5 at 20 °C and 1.0 kPa vapour pressure deficit
	TR	g H_20 h^{-1} m^{-2}	Plant transpiration rate per area at 20 °C and 1.3 kPa vapour pressure deficit
	LAR	leaves $°Cd^{-1}$	Average leaf appearance rate (thermal time, base 0 °C)
Responses	T_{min}	°C	Minimum temperature for leaf elongation
	T_{opt}	°C	Optimum temperature for leaf elongation
	T_{max}	°C	Maximum temperature for leaf elongation
	s_{LER}	kPa^{-1}	Response of leaf elongation rate to vapour pressure deficit
	s_{TR}	kPa^{-1}	Response of transpiration rate to vapour pressure deficit

at which the normalized LER equals zero, T_{opt} is the temperature at which the normalized LER is maximal, and T_{max} is the supra-optimal temperature at which the normalized LER equals zero (all temperatures in °C; see Table 1 for a full list of definitions of traits). Equation (1) was compared with a beta function (Wang and Engel, 1998) and an Arrhenius-type function (Parent and Tardieu, 2012); Supplementary Fig. S2). Regressions were performed using the BFGS method of the "optim" function in the R software (www.r-project.org). The goodness of fit of the three equations was evaluated using the root mean-squared error and models were compared using the Akaike information criterion (AIC; Akaike, 1974) and the Bayesian information criterion (BIC; Schwarz, 1978).

Responses of leaf elongation rate and transpiration to vapour-pressure deficit

The responses of LER and transpiration to leaf–air VPD were calculated during the day in scenario 1 only, with LER being measured as described above. Transpiration rate (TR) was calculated from the weight loss of each pot divided by the total leaf (sheath + blade) area. Direct evaporation from the soil was estimated by measuring the weight loss of pots containing artificial plants, which were watered to maintain a soil water potential similar to that of the pots containing real live plants. The weight of each pot was measured every minute, and then the average was calculated and stored every 15 min.

The LER of the youngest growing leaf measured at the 15 min intervals was first expressed with units of thermal time in order to remove the effects of temperature. It was then averaged over the period of stabilized VPD (i.e. the last 4 h of the 6-h period) and then normalized by the mean TR during those 4 h to remove the effects of plant size and leaf area. The normalized LER and TR data were then fitted with a linear model constrained to 1 at the reference VPD, so that only one parameter described each response, the sensitivities to VPD of LER (sLER, kPa^{-1}) and TR (sTR, kPa^{-1}).

Traits linked to rates of development, leaf expansion, and transpiration

The progress of plant development on the main stem was determined from the leaf stage (LS), adapted from Haun (1973):

$$LS = n + \frac{l}{L} \quad (2)$$

where n is the number of ligulated leaves, l is the exposed length of leaf n+1 at the time of measurement, and L is the final length of the blade of leaf n+1. The exposed length of a leaf was measured with a ruler as the distance from leaf tip to the upper collar of the sheath tube. LS was determined on all plants in scenario 1 from the day before to the last of the LER measurements. The rate of leaf appearance (LAR, leaves $°Cd^{-1}$; inverse of the phyllochron) was calculated as the slope of the relationship between LS and thermal time (base 0 °C).

Because the elongation of leaf 5 was measured during at least one night for all the accessions, the absolute LER of all accessions was compared based on the LER of leaf 5 (LERm, mm h^{-1}) measured at 20 °C, 2–3 d after leaf appearance (i.e. when LER was at its maximum value). The transpiration rate at 20 °C and VPD=1.3 kPa was calculated as the mean of absolute transpiration rate as measured on each of the four nights during the 4-h period of stabilised VPD. At the end of the 4-d period, the whole-plant leaf area was measured (see below). The transpiration rate per unit leaf area (TR, g cm^{-2} h^{-1}) was then calculated by first deducting the evaporation recorded in pots with artificial plants, and then dividing by the whole-plant leaf area.

Traits linked to plant structure

All plant structural traits were measured after the fourth day of LER and TR measurements. The total number of leaves per plant (TL, leaf $plant^{-1}$) was counted. The leaf blades and sheaths of the main stem and tillers were then separated and their lengths, widths, and surface areas were measured using an electronic planimeter (LI-3100C, LI-COR) and used to calculate various traits linked to plant structure. The total leaf area per plant was calculated (LAT, cm^2 $plant^{-1}$). The length-to-width ratio (rlw2, dimensionless) and surface area (LA2, cm^2 $plant^{-1}$) of the blade of main-stem leaf 2 were calculated as proxies of early plant vigour (Rebetzke *et al.*, 2004). It was correlated with seed size (Supplementary Fig. S3). We also determined the slope of the relationship between main-stem individual leaf-blade surface area and leaf rank normalized by the surface area of the blade of leaf 2 (sLAK, dimensionless), and the ratio of leaf-blade to total leaf (sheath + blade) surface area (rLA, dimensionless).

The main-stem leaf blades and sheaths of each plant were pooled and oven-dried at 85 °C until they reached constant mass. The dry mass of the samples was measured and specific leaf mass (mass per leaf area, MLA; g DM cm^{-2} leaf) was calculated by dividing total plant dry mass by the total leaf area, LAT. The samples were then milled and their total N concentration (N mass per unit dry mass) was determined using the Dumas combustion method (Horwitz, 1980) using a FlashEA 1112 N/Protein

Analyzer (ThermoFisher Scientific) and the mass of N per plant was calculated (PN, g N plant^{-1}). Specific leaf N (SLN, g N m^{-2} leaf) was calculated by dividing PN by the total leaf area of the plant.

Data analyses

All data analyses were carried out using the R software (www.r-project.org). ANOVAs on each variable were performed with the function *aov*, considering species as factors and genotypes as replicates. Confidence intervals of differences between means of pairs of species were calculated using a Tukey test (R function *TukeyHSD*) and the significance of these differences were calculated with the function *HSD.test* with α=0.05.

The procedure for building correlograms consisted of the following steps: (i) normality Shapiro–Wilk test; (ii) calculation of Spearman correlations; and (iii) calculation of *q*-values (*P*-value corrected for false-discovery rate). Significant correlations were considered at q<0.01. To compare the intra- versus interspecific variability of each trait, we calculated the ratio of the corresponding coefficient of variation of standard deviation.

Principal component analyses (PCAs) were performed using the function *PCA* of the *FactorMineR* R package (Lê *et al.*, 2008). We considered several sets of traits (e.g. all traits, or traits linked to sensitivities to temperature and VPD only), with data at the accession level. Values of each species on the first five axes of the PCA were determined by calculating the barycentre of all accessions in each species. A hierarchical clustering on principal components (HCPC) analysis of species was then performed based on these first five axes of the PCA using the *HCPC* function of the *FactorMineR* package. In the case of the analysis of the set of traits comprising only the five traits linked to sensitivities, and because the phenotypic space was then automatically reduced to five dimensions (five variables), the hierarchical clustering analysis was carried out based on these five traits rather than on principal components of the PCA. Approximately unbiased (AU) *P*-values (%) were calculated using the *pvclust* function of the *pv.clust* R package, with 1000 bootstrap replications.

Results

Interspecific variability of traits related to plant structure and rates of development, leaf expansion, and transpiration, and their response to temperature and VPD

We measured nine traits related to plant structure and three traits related to the rate of plant development and growth in 60 accessions covering a wide genetic diversity in 12 groups (five accessions in each group) of wheat-related species and subspecies (Fig. 1). Traits related to the rates of plant development and growth (LAR, LERm) and plant size (LA2, LAT, and PN) showed a high variability and significant differences between species (Fig. 3, see Supplementary Tables S3 and S4 for results of ANOVA and for comparisons of intra- versus interspecific variations, respectively). Among these traits, LAR increased with ploidy level (Fig. 3L, P<0.001), while LA2, LAT, and PN were higher for the diploid species than for the polyploid species ($2n > 4n > 6n$; Fig. 3A, D, H; all P<0.001). Traits linked to plant structure but not expected to be linked to plant size (i.e. rlw2, rLA, and sLAK) showed no clear patterns with ploidy (Fig. 3B, F, G), and the other traits (TL, SLN, and TR) also showed no clear pattern. MLA and SLN both showed low overall variability compared to the other traits that we measured.

We examined the sensitivities of LER to temperature and VPD in the 60 accessions. Each night, a temperature between 4 °C and 36 °C was applied for 6 h together with a period of 6 h at the reference temperature of 20 °C (Supplementary Fig. S1). An example for *T. turgidum* subsp. *durum* cultivar Brumaire is shown in Fig. 2, where temperature was first maintained at 20 °C for 6 h and then increased to 24 °C. The LER oscillated around 4 mm h^{-1} during the first period and then increased rapidly to ~5 mm h^{-1} when temperature was increased (Fig. 2C). We normalized the LER measured at the tested temperature by that measured at the reference temperature on the same night in order to examine the effect of the temperature change regardless of differences in LER due to differences in leaf rank or time since leaf emergence (Fig. 4A). We fitted the data to three different function equations to estimate the cardinal temperatures of LER, namely a beta function (Wang and Engel, 1998), an Arrhenius function (Parent and Tardieu, 2012), and a segmented linear equation (Eqn 1). For all accessions, the segmented linear equation provided the best fit (Supplementary Fig. S2, Supplementary Table S5), and all data were therefore analysed using this model (Fig. 4A provides an example of the type of response we obtained).

The three cardinal temperatures showed moderate but significant variability between the 12 groups of species and subspecies (Fig. 4D–F), with T_{min} ranging from –1.7 °C to 3.9 °C, T_{opt} from 24.0 °C to 31.6 °C, and T_{max} from 36.2 °C to 53.4 °C (see Supplementary Tables S6 and S7 for values at the accession and species level, respectively). There was no clear pattern between ploidy levels, genomes, or between wild versus domesticated species.

We quantified the responses of LER and TR to VPD during the day using an approach similar to that described above for the response of LER to temperature during the night. Each day, a VPD between 0.5 kPa and 3.0 kPa was applied for 6 h together with a period of 6 h at the reference VPD of 1.3 kPa. Examples of time-courses we obtained for LER and transpiration are shown in Fig. 2C, D. LER oscillated around 5.5 mm h^{-1} at the reference VPD and decreased to ~4 mm h^{-1} when VPD was increased to 2.7 kPa. At the same time, transpiration rate, which stabilized at 13 g h^{-1} at the reference VPD, increased to 19 g h^{-1}. LER and TR (plant transpiration rate per area) at the tested values of VPD were normalized by their corresponding value at the reference VPD to remove the effects of leaf rank, time since leaf emergence, and plant leaf area. Both responses to VPD were fitted with a linear model, the slope of which is the sensitivity of LER (sLER) or TR (sTR) to VPD (Fig. 4B, C). sLER showed significant variability between species and subspecies (Fig. 4G), ranging from –0.268 kPa^{-1} to –0.037 kPa^{-1}, while sTR (Fig. 4H) showed lower variability (Supplementary Tables S6, S7). However, at the level of single traits, we did not observe any clear patterns between the 12 groups of species.

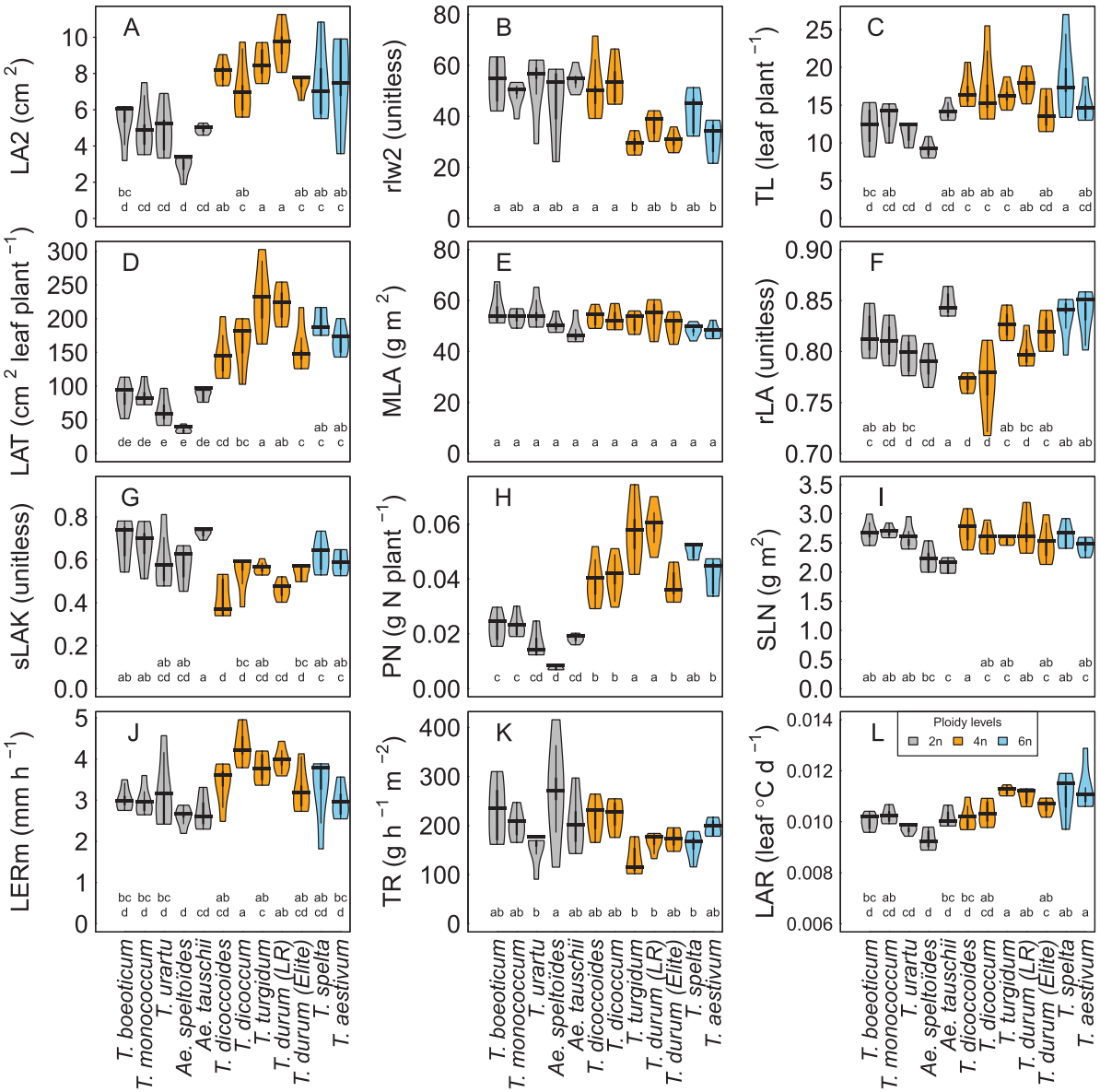

Fig. 3. Traits related to plant structure and rate of development, leaf expansion, and transpiration for the 12 groups of wheat-related species and subspecies. (A) Surface area of leaf 2 (LA2), (B) length-to-width ratio of leaf 2 (rlw2), (C) total number of leaves per plant (TL), (D) total leaf surface area per plant (LAT), (E) specific leaf mass (mass per leaf area, MLA), (F) ratio of leaf blade to total leaf surface area (rLA), (G) slope of leaf blade surface area versus leaf rank, normalized by the surface area of leaf 2 (sLAK), (H) total N mass per plant (PN), (I) specific leaf N (SLN), (J) leaf elongation rate of leaf 5 at 20 °C and vapour-pressure deficit (VPD) of 1.0 kPa (LERm), (K) transpiration rate at 20 °C and 1.3 kPa VPD (TR), and (L) leaf appearance rate (LAR; thermal time, base 0 °C). Data are means (±SD) for n=5 accessions. *Triticum turgidum* subsp. *durum* was separated in two groups: landrace (LR) populations grown before the Green Revolution and elite cultivars released afterwards.

Ploidy level, phylogeny, and breeding together explain the phenotypic space of all traits

An understanding of the structure of the interspecific diversity and how the intraspecific diversity is nested inside is made possible by considering the multi-dimensional space constituted by all traits together (the 'phenotypic space'). We found significant correlations between most traits (Fig. 5, Supplementary Table S8). The strongest positive correlations were between traits related to plant structure and plant size, but we also found significant correlations between traits of different types, for example between response traits and traits related to plant structure.

We used principal component analyses (PCAs) to reduce the number of dimensions of the phenotypic space to five. PCA based on all traits at the accession level (Fig. 6A–D) showed that within each group of species, the diversity of values for the first three components was low compared to the overall diversity observed at the interspecific level (Fig. 6B, D). The first principal component (PC1) explained

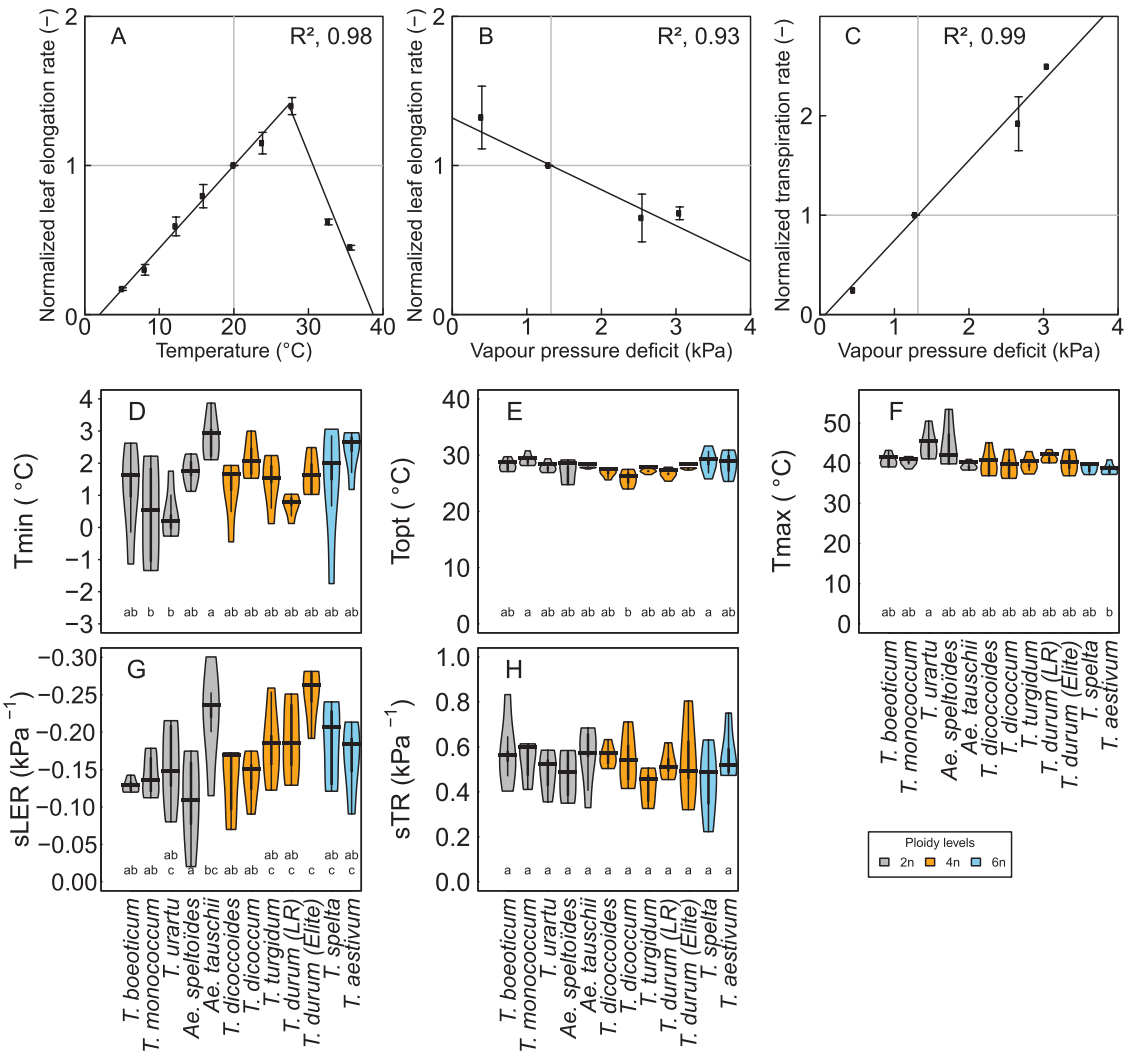

Fig. 4. Typical responses of leaf elongation rate (LER) and transpiration rate (TR) to temperature and vapour-pressure deficit (VPD), and variation in cardinal temperatures and sensitivities of LER and TR to VPD across the 12 groups of wheat-related species and subspecies. (A, B) Normalized LER versus (A) temperature of the leaf growth zone and (B) VPD, and (C) normalized TR versus VPD for *Triticum turgidum* subsp. *durum* cultivar Neodur. Data are means (±SD) for n=6 independent replicates, except for temperatures <12 °C and >28 °C where n=3. The black lines are linear (A, C) or segmented-linear (C) regressions, and the grey horizontal and vertical lines indicate the normalization point constraining the fitted function equations. (D) Minimum (T_{min}), (E) optimum (T_{opt}), and (F) maximum (T_{max}) temperatures for LER of the leaf meristematic zone for the 12 groups of wheat-related species and subspecies. (G, H) Variability of the sensitivity of (G) LER (sLER) and (H) TR (sTR) to VPD. Data in (D–H) are means (±SD) for n=5 accessions. *Triticum turgidum* subsp. *durum* was separated in two groups: landrace (LR) populations grown before the Green Revolution and elite cultivars released afterwards.

30% of the observed variance and was mainly explained by traits related to development rate (e.g. LAR and LERm) and traits linked to plant size (e.g. LAT and TL; Fig. 6A), and it discriminated diploid species from tetraploid and hexaploid species (Fig. 6B). Diploid species had a smaller leaf 2 area (LA2), lower leaf appearance rate (LAR), fewer leaves (TL), and a lower total leaf area per plant (LAT) compared with tetraploid and hexaploid species (Fig. 3). However, because most of the wild species used in this study were diploids, and because *T. turgidum* subsp. *dicoccoides* was close to the origin of PC1, we are not able to conclude if this axis discriminated species based on domestication or on ploidy level.

The hierarchical clustering on principal components (HCPC) analysis based on the first five components of the PCA classified the 12 groups into six clusters (Fig. 6E). The first branching of the dendogram (corresponding to the highest relative distance) separated the diploid and polyploid species. For the diploids, the second order of the dendrogram separated genome A from the other two diploid genomes, whilst for the polyploids it separated *T. turgidum* subsp. *dicoccoides* and subsp. *dicoccum* from the other polyploid species. The third order of

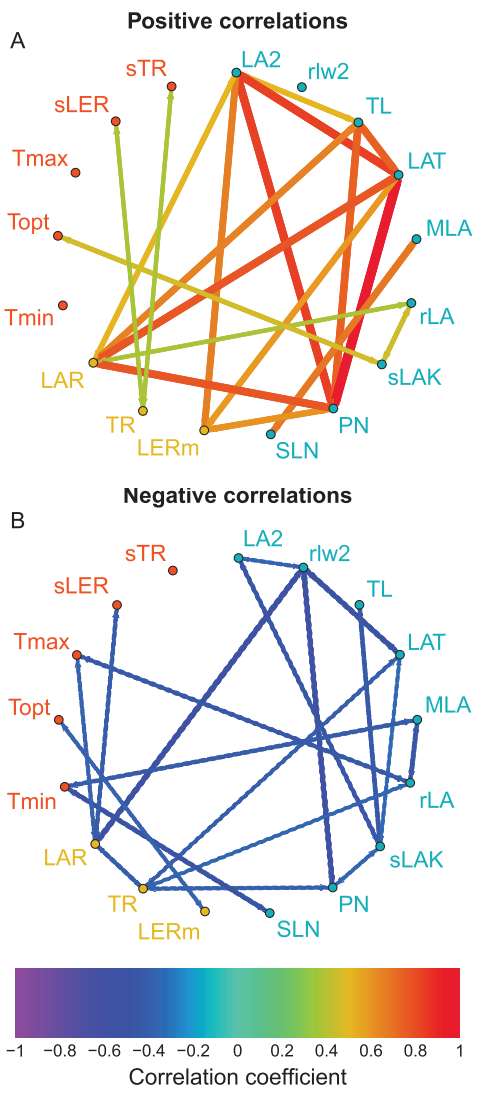

Fig. 5. Correlograms of Spearman's correlation coefficients between traits at the accession level across the 12 groups of wheat-related species and subspecies. See Table 1 for definitions of variables. (A) Positive correlations and (B) negative correlations. Traits in blue are related to plant structure, those in yellow are related to absolute rates of development, expansion, or transpiration, and those in red are related to the responses of LER to temperature and VPD, and of TR to VPD. The colour and thickness of the lines indicate the value of the correlation coefficient. Only significant correlations are shown (q-value<0.01).

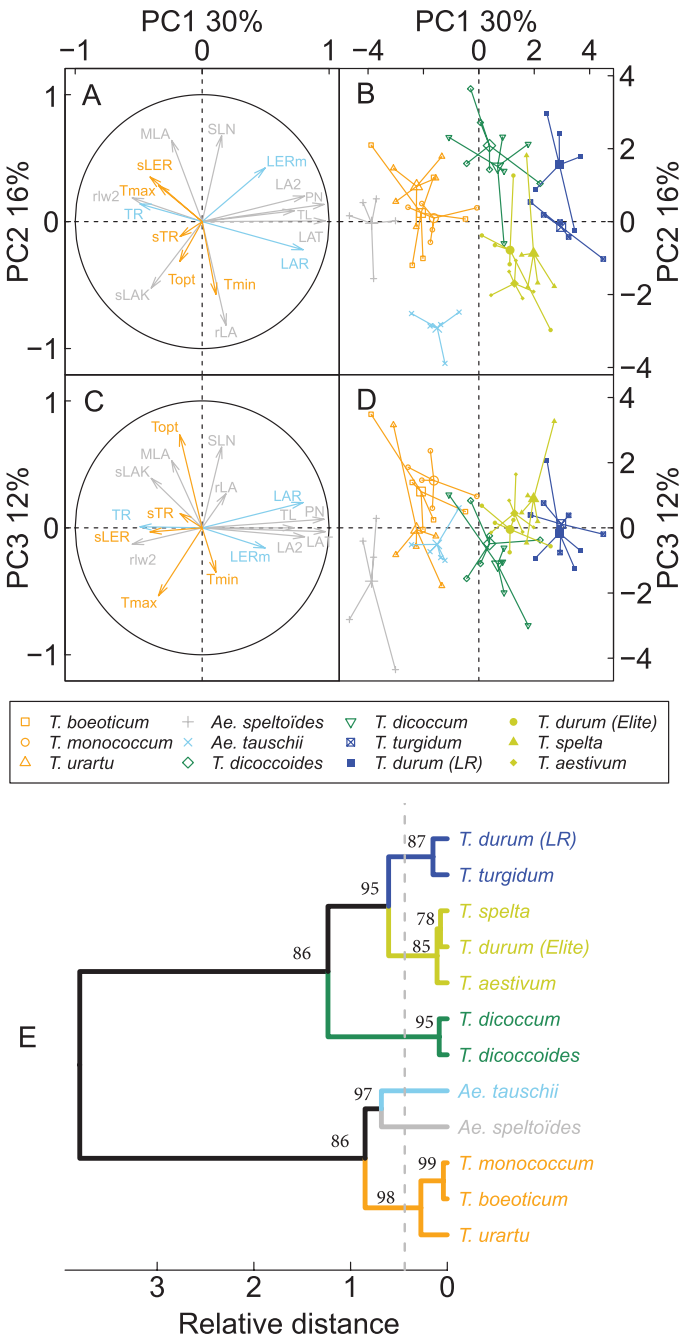

Fig. 6. Principal component analysis (PCA) and hierarchical clustering on principal components (HCPC) analysis for the 17 traits measured for the 60 accessions across the 12 groups of wheat-related species and subspecies. See Table 1 for definitions of variables. (A, C) Representation of structural traits (grey), absolute rates of development, expansion, and transpiration (blue), and responses of leaf elongation rate to temperature and vapour-pressure deficit (VPD), and of transpiration rate to VPD (orange) for (A) PC1 versus PC2 and (C) PC1 versus PC3. (B, D) Factor maps of the accessions and the barycentre of each cluster identified by the HCPC analysis corresponding to (A) and (B), respectively. (E) Dendrogram of the HCPC analysis performed on the barycentre of each species in the first five axes of the PCA. The dashed vertical line shows the threshold of relative distance for clustering species. The numbers indicate the approximately unbiased (AU) P-value obtained from 1000 bootstrap replications.

clustering grouped together *T. turgidum* subsp. *durum* elite cultivars and the two hexaploid species (*T. aestivum* subsp. *aestivum* and subsp. *spelta*), while *T. turgidum* subsp. *durum* landraces were grouped with *T. turgidum* subsp. *turgidum*. The wild and cultivated emmer wheat species (*T. turgidum* subsp. *dicoccoides* and subsp. *dicoccum*) were grouped together. Thus, the phenotypic space based on the 17 traits that we studied discriminated wheat-related species and subspecies based on their ploidy level, domestication, and breeding, and the resulting clustering of species fitted well with the phylogeny of the 12 groups of species and subspecies.

Phylogeny structures the phenotypic space of traits related to the rate of plant development and growth, and their responses to temperature and VPD

We conducted a similar analysis combining PCA and HCPC analysis but based on traits linked to plant structure only (Supplementary Fig. S4) and obtained similar results to when all 17 traits were used (with marginal differences), suggesting that the structure traits drove the clustering of the 12 groups of species. We therefore performed a similar analysis on traits linked to rates and sensitivities whilst excluding structure traits (Fig. 7). The first axis discriminated species with high LAR from those with low TR, sLER, and T_{max}, while the second axis discriminated species with high T_{max} from those with low T_{min}, T_{opt}, and sTR. T_{opt} was negatively correlated with LERm (Supplementary Table S8) and these were the main contributing traits to the third axis. The resulting HCPC analysis first segregated two groups (Fig. 7E). The first consisted of the cultivated tetraploid and hexaploid species, as well as *Ae. tauschii*, while the second consisted of the wild and cultivated diploids and the wild tetraploid species *T. turgidum* subsp. *dicoccoides*. Within these two groups, the HCPC analysis produced a few unexpected results, with *T. turgidum* subsp. *dicoccoides* clustered with *T. monococcum* (subsp. *monococcum* and subsp. *beoticum*), *T. aestivum* subsp. *spelta* clustered with a group of three *T. turgidum* subspecies, and *Ae. tauschii* in the same cluster as *T. aestivum* subsp. *aestivum*. Overall, these results indicated that the rate of development of growth and the sensitivities to temperature and VPD are well-conserved, with low variability within species compared to the phenotypic space of wheat-related species, and that their interspecific variability is mainly structured by phylogeny.

Finally, we analysed the structure of the phenotypic space of response traits only, knowing that the values of individual traits did not show any clear trends (Fig. 4). Because we only measured five response traits, the phenotypic space was automatically reduced to five dimensions (five variables), which appeared as independent in the PCA (Fig. 8A), we then performed a hierarchical clustering analysis based on these five traits. The resulting dendogram again showed clear patterns (Fig. 8E). The clustering first segregated two wild diploid species, *Ae. speltoïdes* and *T. uratu*, from the other species, indicating that they had significantly different responses to temperature and evaporative demand. Apart from this, the analysis clustered three other groups, the first of which comprised all tetraploid species, regardless of wild/domesticated subgroups, the second group contained the two wild and domesticated *T. monococcum* species (subsp. *monococcum* and *boeticumm*, respectively), and the third group contained the two hexaploid species (*T. aestivum* subsp. *spelta* and subsp. *aestivum*) and *Ae. tauschii*, that is, all species with a D genome. This analysis therefore indicated that the interspecific variability in temperature and VPD responses was structured by both the ploidy level and the phylogenetic relationships. However, domestication and/or breeding pressure does not appear to have played a role in modifying these responses..

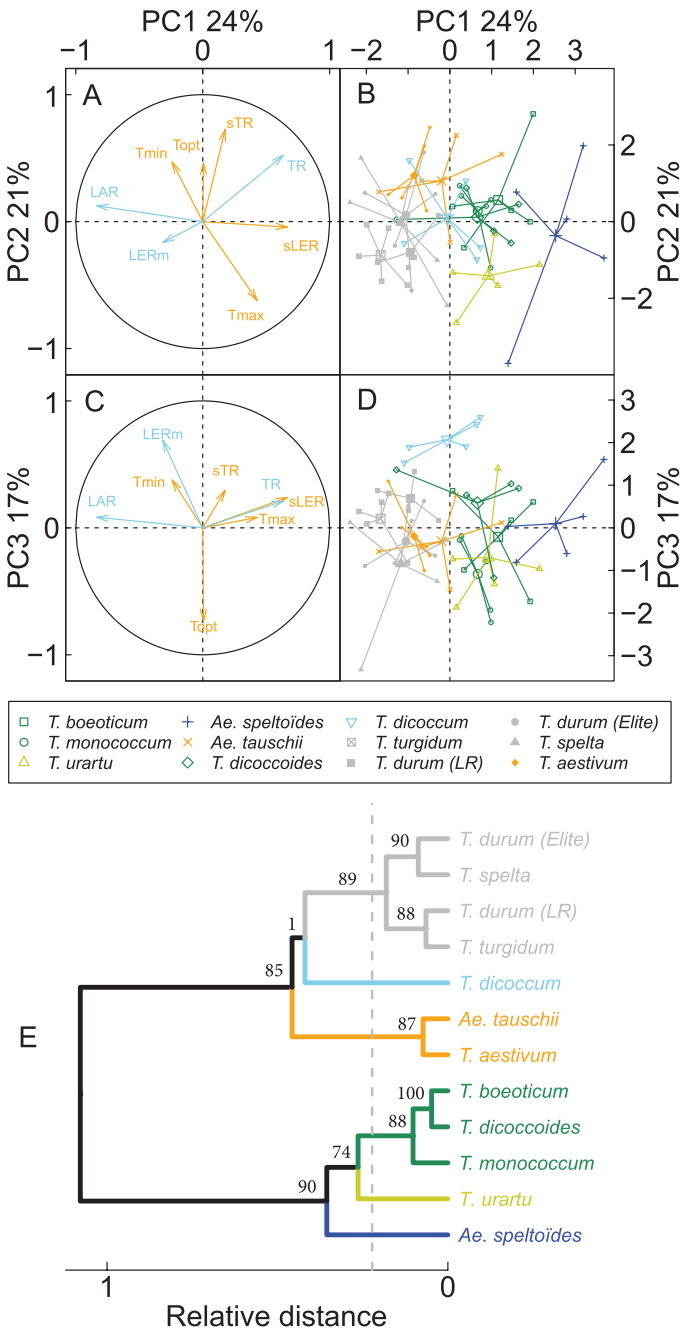

Fig. 7. Principal component analysis (PCA) and hierarchical clustering on principal components (HCPC) analysis for the traits related to the absolute rates of development, expansion and transpiration, and response to temperature and vapour-pressure deficit (VPD) for the 60 accessions across the 12 groups of wheat-related species and subspecies. See Table 1 for definitions of variables. (A, C) Representation of absolute rates of development, expansion, and transpiration rate (blue) and responses of leaf elongation rate to temperature and VPD, and transpiration rate to VPD (orange) for (A) PC1 versus PC2 and (C) PC1 versus PC3. (B, D) Factor maps of the accessions and the barycentre of each cluster identified by the HCPC analysis corresponding to (A) and (B), respectively. (E) Dendrogram of the HCPC analysis performed on the barycentre of each species in the first five axes of the PCA. The dashed vertical line shows the threshold of relative distance for clustering species. The numbers indicate the approximately unbiased (AU) *P*-value obtained from 1000 bootstrap replications.

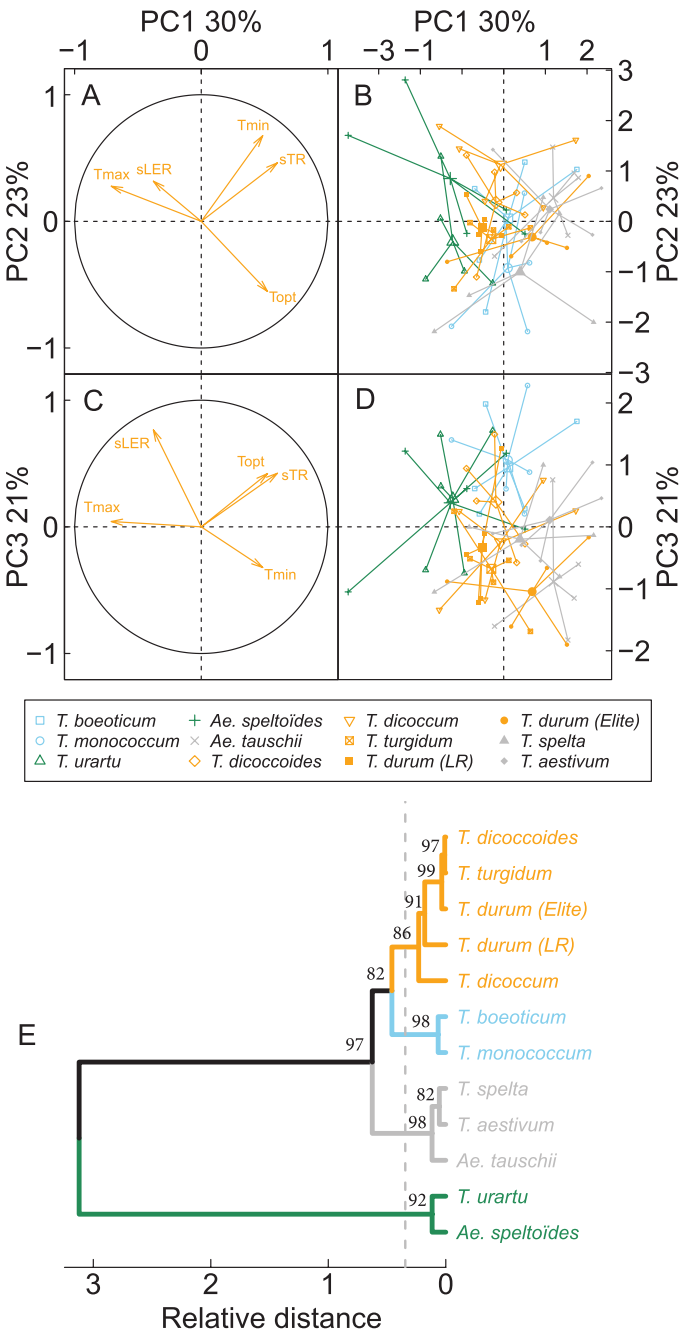

Fig. 8. Principal component analysis (PCA) and hierarchical clustering on principal components (HCPC) analysis based on trait values related to response to temperature and vapour-pressure deficit (VPD) for the 60 accessions across the 12 groups of wheat related species and subspecies. See Table 1 for definitions of variables. (A, C) Representation of the response of leaf elongation rate to temperature and VPD, and transpiration rate to VPD for (A) PC1 versus PC2 and (C) PC1 versus PC3. (B, D) Factor maps of the accessions and the barycentre of each cluster identified by the HCPC analysis corresponding to (A) and (B), respectively. (E) Dendrogram of the HCPC analysis performed on the barycentre of each species in the five variables. The dashed vertical line shows the threshold of relative distance for clustering species. The numbers indicate the approximately unbiased (AU) *P*-value obtained from 1000 bootstrap replications.

Discussion

Modelling the sensitivities of leaf elongation and transpiration rates to temperature and vapour pressure deficit for a large genetic diversity

The responses of expansion processes of plant organs to temperature have been studied extensively (reviewed in Parent *et al.*, 2012). Most of these studies have concluded that the response is similar to that of plant development, and the few studies that have assessed intraspecific variability have suggested that it is low (Parent and Tardieu, 2012). The result is that most crop models use similar formalisms and parameter values for both the response of development and expansion processes without including genetic variability in these parameters (Parent and Tardieu, 2014). A range of formalisms are used in crop models, from the simplest linear model to more complex, curvilinear models (Kumudini *et al.*, 2014; Parent and Tardieu, 2014; Wang *et al.*, 2017). In this study, we used a segmented linear formalism, which provided an adequate fit to the observed sensitivities in 60 accessions of wheat-related species (Supplementary Fig. S2, Supplementary Table S6). As expected, the observed intraspecific variability was low (Supplementary Tables S4, S6), and so was the interspecific variability (albeit not zero; see below, Fig. 4, Supplementary Table S4). This indicates that a modelling strategy based on parsimony with a single set of parameter values for all wheat-related species is probably a good strategy (Parent *et al.*, 2016). Such a model with no genotypic variation would be probably very close to one that assumes organized genetic variation, but would have the advantage of avoiding time-consuming experiments on each individual wheat accession.

To our knowledge, there have been no studies to date that have assessed the response of leaf elongation to VPD in wheat. This is despite the fact that most cereal species react strongly to changes in evaporative demand, and large genetic variability in the response of LER to VPD has been found in the species in which it has been studied (e.g. Parent *et al.*, 2010b; Welcker *et al.*, 2011). Here, we have demonstrated that a linear model can fit this response across a large diversity of wheat-related species. The range of sensitivities at the interspecific level (from –10% to –25% kPa^{-1}; Fig. 4G) was very close to that observed in maize (Welcker *et al.*, 2011; Lacube *et al.*, 2017). Given that consideration of this response can greatly improve prediction of leaf area in contrasting field sites for maize, we would also expect it to be the case in wheat growth predictions.

Although the response of transpiration to VPD has been investigated in many species including bread wheat (e.g. Schoppach and Sadok, 2012; Schoppach *et al.*, 2012), and very high variability has been found across generations of selections of Australian wheat (Schoppach *et al.*, 2016), there has been no information about its variability in wheat-relative species. Unexpectedly, the variability of responses observed in this study was very low at both the intra- and interspecific level

compared to that found in 23 cultivars released from 1890 to 2010 in Australia (Fig. 4H, Supplementary Tables S4, S6; Schoppach *et al.*, 2016). For some genotypes, Schoppach *et al.* (2012) observed a break-point in the TR–VPD relationship between 2.4 kPa and 3.9 kPa, whereas in the range of VPDs that we tested a linear model fitted the response of all accessions without any break-point (Fig. 4C). This could be explained by the limited range of VPD used here (0.5–3.0 kPa compared with 0.8–4.5 kPa in Schoppach *et al.*, 2012), which corresponded to the environmental range observed in the spring in most temperate regions.

Most traits have probably evolved slowly, following polyploidization, phylogeny, and breeding pressure

A striking result of this study was the fact that a hierarchical clustering of species based on traits that have not been directly selected was able to reproduce almost perfectly the known phylogeny of wheat-related species and subspecies. Our hierarchical clustering based on traits linked to plant structure discriminated diploid from polyploid species, regardless of domestication (e.g. *T. mococcum* subsp. *mococcum* and subsp. *boeoticum* clustered together, and *T. turgidum* subsp. *dicoccoides* and subsp. *dicoccum* clustered together; Fig. 6, Supplementary Fig. S4). This suggests a specific effect of ploidy on plant physiology, such as that observed in trees (De Baerdemaeker *et al.*, 2018). In addition, we found variations depending on the genome, with different sets of trait values between diploid species with genome A, D, or S (Figs 1, 6, Supplementary Fig. S4. Finally, selection pressure seems to have affected these traits (but much less than phylogeny and ploidy), with different clusters of trait values for the earliest tetraploid species (*T. turgidum* subsp. *dicoccoides* and subsp. *dicoccum*) and landraces of *T. turgidum* subsp. *durum* selected before the Green Revolution, compared with durum wheat cultivars released later.

At the level of individual traits, the values of the five traits related to sensitivities to temperature and VPD did not indicate any clear patterns, with no obvious impact of selection pressure, domestication, genome or sub-genome, ploidy, or phylogenetic links between species (Fig. 4). In contrast, a clustering based on these traits did show clear patterns, with an effect of both ploidy and phylogenetic relationships (Fig. 8). Overall, species that were phylogenetically close showed similar phenotypic spaces, indicating that these traits are well-conserved and have probably evolved slowly, following phylogeny, as has been proposed previously for the response to temperature in a much wider genetic diversity of cultivated plants (Parent and Tardieu, 2012).

What sources of genetic improvement are available within species and between related species?

In addition to providing formalisms and parameter values for process-based models, we also hypothesized that our study could identify new sources of genetic diversity for the responses of LER and TR to VPD and temperature within wheat-related species, in particular in wild or cultivated *T. turgidum* or diploid species, which could then potentially enrich the genetic diversity of cultivated wheat via the use of a synthetic-wheat strategy.

Most synthetic-derived wheat cultivars have been developed by crossing *Ae. tauschii* with elite durum wheat cultivars, and more recently with *T. dicoccoides*, *T. dicoccum*, or *T. turgidum* (Singh and Trethowan, 2008; Li *et al.*, 2018; Rosyara *et al.*, 2019). Several studies have reported significant improvements in heat and drought tolerance of bread wheat cultivars derived from *Ae. tauschii* × *T. durum* crosses compared with locally adapted elite cultivars (e.g. Lopes and Reynolds, 2011; Mariano Cossani and Reynolds, 2015). However, the interspecific variability of wild and cultivated wheat-related species for traits related to temperature and evaporative demand has not yet been explored.

As expected, our results showed that the genetic variability of structural traits observed within wheat ancestors or the secondary gene pool was very different from that observed in modern durum or bread wheat cultivars, and mostly presented lower values (Fig. 3), which would not be advantageous in an agronomic context. A source of enrichment of genetic diversity for these traits therefore needs to be sought in other wild species. In contrast, for response traits, some wild relative species or wheat ancestors might provide adaptive value if introduced into cultivated wheat species (Figs 4, 8).

The responses of LER and TR to temperature or VPD in *Ae. tauschii* and *T. dicoccum* were similar to those of *T. aestivum* (Figs. 4, 8). In particular, accessions of *Ae. tauschii* presented very similar trait values compared to modern wheat lines and they delimitated a phenotypic space that was almost nested in that of *T. aestivum* (Fig. 8E). In contrast, *T. uratu* and *Ae. speltoïdes* showed very distinct responses and had higher T_{max} and lower sLER than elite bread and durum wheat cultivars (Fig. 4). Synthetic tetraploid and hexaploid lines have been created with *T. urartu* and *Ae. speltoïdes* but, to our knowledge, they have not been evaluated for their responses to temperature or evaporative demand (Valkoun, 2001; Kishii, 2019). Although introgressions from these species within wheat is practically and methodically challenging, recent developments of genomic resources and biotechnology have good potential to accelerate the use of diploid wheat-related species other than *Ae. tauschii* (Brunazzi *et al.*, 2018). Several studies have focused on the responses of vegetative and/or reproductive traits to high temperature in *Aegilops* species, and genetic variability at both the intra- and interspecific levels has been observed (Pradhan *et al.*, 2012). Although we considered only a very limited number of accessions in each species, our results suggest that *T. urartu* and *Ae. speltoïdes* could be interesting sources of genes to develop wheat cultivars that are able to maintain high LER under high temperature and evaporative demand.

Conclusions

In addition to providing new formalisms for trait responses together with model parameters for 12 wheat-related species and subspecies, this study indicates that traits linked to the responses of LER and TR to temperature and VPD are well-conserved, with an unexpected low genetic variability within species. Our results suggest that vegetative traits have probably evolved slowly, following phylogenetic links between accessions, and that both domestication and phylogenetic relationships have driven the slow evolution of temperature and VPD responses. Finally, the study has identified potential sources for varietal improvement that currently reside in wheat-related species.

Supplementary data

The following supplementary material is available at *JXB* online.

Fig. S1. Scenarios of temperature and vapour pressure deficit applied in the experiments.

Fig. S2. Normalized leaf elongation rate versus temperature of the leaf growth zone fitted using three different non-linear models.

Fig. S3. Relationship between the area of leaf 2 and individual grain weight.

Fig. S4. Principal component analysis and hierarchical clustering analysis for traits related to plant structure for the 12 studied species.

Table S1. List of the 60 accessions that were studied.

Table S2. Alleles of major genes for photoperiod response, cold requirement, and reduced height, together with predicted phenotypes for the 60 accessions that were studied.

Table S3. Results of the ANOVAs for each of the 17 traits measured in the study.

Table S4. Intra- and inter-specific values of coefficient of variation for the 17 traits measured in the study.

Table S5. Comparison of the three non-linear models fitted to the leaf elongation rate versus temperature of the leaf growth zone.

Table S6. Estimated cardinal temperatures of the leaf elongation rate response to temperature together with sensitivities of LER and transpiration rate to VPD for each of the 60 accessions that were studied.

Table S7. Estimated cardinal temperatures of leaf elongation rate response to temperature together with sensitivities of LER and transpiration rate to VPD for each of the 12 groups of wheat-related species.

Table S8. Matrix of Spearman's correlation coefficients between the 17 traits measured in the study.

Acknowledgements

SL was supported by a Convention Industrielle de Formation par la Recherche (CIFRE convention no. 2017/1069) between ANRT and ITK. The authors thank François Balfourier (UMR GDEC, INRAE, Clermont-Ferrand, France) and Pierre Roumet (UMR AGAP, INRAE, Montpellier, France) for advice on selecting the material and for providing seeds, and Dr Jacques Le Gouis and Ms S. Rougeol (UMR GDEC, INRAE, Clermont-Ferrand, France) for genotyping the major genes for the accessions used in this study.

Author contributions

BP and PM designed the research; SL, BP, and PM designed the experiments; SL performed the experiments; SL, BP, and PM analysed the data; BP wrote the first draft of the manuscript; all authors contributed to the revision of the manuscript.

Data availability

The data that support the findings of this study are openly available in Zenodo at https://zenodo.org/record/5511805; Leveau *et al.*, (2021).

References

Akaike H. 1974. A new look at the statistical model identification. IEEE Transactions on Automatic Control **19**, 716–723.

Allahverdiyev TI. 2015. Physiological traits of durum wheat (*Triticum durum* Desf.) and bread wheat (*Triticum aestivum* L.) genotypes under drought stress. Agricultural Sciences **6**, 848–859.

Ben-Ari T, Boé J, Ciais P, Lecerf R, Van der Velde M, Makowski D. 2018. Causes and implications of the unforeseen 2016 extreme yield loss in the breadbasket of France. Nature Communications **9**, 1627.

Brunazzi A, Scaglione D, Talini RF, Miculan M, Magni F, Poland J, Enrico Pè M, Brandolini A, Dell'Acqua M. 2018. Molecular diversity and landscape genomics of the crop wild relative *Triticum urartu* across the Fertile Crescent. The Plant Journal **94**, 670–684.

Comai L. 2005. The advantages and disadvantages of being polyploid. Nature Reviews Genetics **6**, 836–846.

Curtis BC. 2002. Wheat in the world. In: Curtis BC, Rajaram S, Macpherson HG. eds. Bread wheat improvement and production. Plant Production and Protection Series, 30. Rome: FAO, 1–18.

Davies WJ, Wilkinson S, Loveys B. 2001. Stomatal control by chemical signalling and the exploitation of this mechanism to increase water use efficiency in agriculture. New Phytologist **153**, 449–460.

De Baerdemaeker NJF, Hias N, Van den Bulcke J, Keulemans W, Steppe K. 2018. The effect of polyploidization on tree hydraulic functioning. American Journal of Botany **105**, 161–171.

Giunta F, Pruneddu G, Zuddas M, Motzo R. 2019. Bread and durum wheat: intra- and inter-specific variation in grain yield and protein concentration of modern Italian cultivars. European Journal of Agronomy **105**, 119–128.

Gorafi YSA, Kim JS, Elbashir AAE, Tsujimoto HA. 2018. Population of wheat multiple synthetic derivatives: An effective platform to explore, harness and utilize genetic diversity of Aegilops tauschii for wheat improvement. Theoretical and Applied Genetics **131**, 1615–1626.

Hammer G, Messina C, Wu A, Cooper M. 2019. Biological reality and parsimony in crop models—why we need both in crop improvement! *in silico* Plants **1**, diz010.

Handmer J, Honda Y, Kundzewicz ZW, *et al.* 2012. Changes in impacts of climate extremes: human systems and ecosystems. In: Field CB, Barros V, Stocker TF, ***et al***. eds. Managing the risks of extreme events and disasters to advance climate change adaptation. Special Report of the

Intergovernmental Panel on Climate Change. Cambridge, UK: Cambridge University Press, 231–290.

Haun JR. 1973. Visual quantification of wheat development. Agronomy Journal **65**, 116.

Hias N, Svara A, Keulemans JW. 2018. Effect of polyploidisation on the response of apple (*Malus* × *domestica* Borkh.) to *Venturia inaequalis* infection. European Journal of Plant Pathology **151**, 515–526.

Horwitz W (ed.). 1980. Dumas method (7.016). In: Official methods of analysis of the Association of Official Analytical Chemists. Washington, DC: AOAC.

Jeuffroy M-H, Casadebaig P, Debaeke P, Loyce C, Meynard J-M. 2014. Agronomic model uses to predict cultivar performance in various environments and cropping systems. A review. Agronomy for Sustainable Development **34**, 121–137.

Kishii M. 2019. An update of recent use of *Aegilops* species in wheat breeding. Frontiers in Plant Science **10**, 585.

Kumudini S, Andrade FH, Boote KJ, *et al.* 2014. Predicting maize phenology: intercomparison of functions for developmental response to temperature. Agronomy Journal **106**, 2087–2097.

Lacube S, Fournier C, Palaffre C, Millet EJ, Tardieu F, Parent B. 2017. Distinct controls of leaf widening and elongation by light and evaporative demand in maize. Plant, Cell & Environment **40**, 2017–2028.

Lê S, Josse J, Husson F. 2008. FactoMineR: a package for multivariate analysis. Journal of Statistical Software **25**, 1–18.

Leveau S, Parent B, Zaka S, Martre P. 2021. Data from: Differential sensitivity to temperature and evaporative demand in wheat relatives. Zenodo https://zenodo.org/record/5511805

Li A, Liu D, Yang W, Kishii M, Mao L. 2018. Synthetic hexaploid wheat: yesterday, today, and tomorrow. Engineering **4**, 552–558.

Lobell DB, Schlenker W, Costa-Roberts J. 2011. Climate trends and global crop production since 1980. Science **333**, 616–620.

Lopes MS, Reynolds MP. 2011. Drought adaptive traits and wide adaptation in elite lines derived from resynthesized hexaploid wheat. Crop Science **51**, 1617–1626.

Mariano Cossani C, Reynolds MP. 2015. Heat stress adaptation in elite lines derived from synthetic hexaploid wheat. Crop Science **55**, 2719–2735.

Marti J, Slafer GA. 2014. Bread and durum wheat yields under a wide range of environmental conditions. Field Crops Research **156**, 258–271.

Martin A, Simpfendorfer S, Hare RA, Eberhard FS, Sutherland MW. 2011. Retention of D genome chromosomes in pentaploid wheat crosses. Heredity **107**, 315–319.

Parent B, Millet EJ, Tardieu F. 2019. The use of thermal time in plant studies has a sound theoretical basis provided that confounding effects are avoided. Journal of Experimental Botany **70**, 2359–2370.

Parent B, Suard B, Serraj R, Tardieu F. 2010a. Rice leaf growth and water potential are resilient to evaporative demand and soil water deficit once the effects of root system are neutralized. Plant, Cell & Environment **33**, 1256–1267.

Parent B, Tardieu F. 2012. Temperature responses of developmental processes have not been affected by breeding in different ecological areas for 17 crop species. New Phytologist **194**, 760–774.

Parent B, Tardieu F. 2014. Can current crop models be used in the phenotyping era for predicting the genetic variability of yield of plants subjected to drought or high temperature? Journal of Experimental Botany **65**, 6179–6189.

Parent B, Turc O, Gibon Y, Stitt M, Tardieu F. 2010b. Modelling temperature-compensated physiological rates, based on the coordination of responses to temperature of developmental processes. Journal of Experimental Botany **61**, 2057–2069.

Parent B, Vile D, Violle C, Tardieu F. 2016. Towards parsimonious ecophysiological models that bridge ecology and agronomy. New Phytologist, **210**, 380–382.

Perego A, Sanna M, Giussani A, Chiodini ME, Fumagalli M, Pilu SR, Bindi M, Moriondo M, Acutis M. 2014. Designing a high-yielding maize ideotype for a changing climate in Lombardy plain (northern Italy). The Science of the Total Environment **499**, 497–509.

Petersen G, Seberg O, Yde M, Berthelsen K. 2006. Phylogenetic relationships of *Triticum* and *Aegilops* and evidence for the origin of the A, B, and D genomes of common wheat (*Triticum aestivum*). Molecular Phylogenetics and Evolution **39**, 70–82.

Pradhan GP, Prasad PVV, Fritz AK, Kirkham MB, Gill BS. 2012. High temperature tolerance in *Aegilops* species and its potential transfer to wheat. Crop Science **52**, 292–304.

Rebetzke GJ, Botwright TL, Moore CS, Richards RA, Condon AG. 2004. Genotypic variation in specific leaf area for genetic improvement of early vigour in wheat. Field Crops Research **88**, 179–189.

Reyer CP, Leuzinger S, Rammig A, *et al.* 2013. A plant's perspective of extremes: terrestrial plant responses to changing climatic variability. Global Change Biology **19**, 75–89.

Rojas M, Lambert F, Ramirez-Villegas J, Challinor AJ. 2019. Emergence of robust precipitation changes across crop production areas in the 21st century. Proceedings of the National Academy of Sciences, USA **116**, 6673–6678.

Rosyara U, Kishii M, Payne T, Sansaloni CP, Singh RP, Braun HJ, Dreisigacker S. 2019. Genetic contribution of synthetic hexaploid wheat to CIMMYT's spring bread wheat breeding germplasm. Scientific Reports **9**, 12355.

Rötter RP, Tao F, Höhn JG, Palosuo T. 2015. Use of crop simulation modelling to aid ideotype design of future cereal cultivars. Journal of Experimental Botany **66**, 3463–3476.

Schoenfelder KP, Fox DT. 2015. The expanding implications of polyploidy. The Journal of Cell Biology **209**, 485–491.

Schoppach R, Fleury D, Sinclair TR, Sadok W. 2017. Transpiration sensitivity to evaporative demand across 120 years of breeding of Australian wheat cultivars. Journal of Agronomy and Crop Science **203**, 219–226.

Schoppach R, Sadok W. 2012. Differential sensitivities of transpiration to evaporative demand and soil water deficit among wheat elite cultivars indicate different strategies for drought tolerance. Environmental and Experimental Botany **84**, 1–10.

Schoppach R, Taylor JD, Majerus E, Claverie E, Baumann U, Suchecki R, Fleury D, Sadok W. 2016. High resolution mapping of traits related to whole-plant transpiration under increasing evaporative demand in wheat. Journal of Experimental Botany **67**, 2847–2860.

Schwarz G. 1978. Estimating the dimension of a model. The Annals of Statistics **6**, 461–464.

Singh RP, Trethowan R. 2008. Breeding spring bread wheat for irrigated and rainfed production systems of the developing world. In: Kang MS, Priyadarshan PM. eds. Breeding major food staples. Oxford, UK: Blackwell Publishing, 107–140.

Tardieu F. 2012. Any trait or trait-related allele can confer drought tolerance: just design the right drought scenario. Journal of Experimental Botany **63**, 25–31.

Tardieu F, Parent B. 2017. Predictable 'meta-mechanisms' emerge from feedbacks between transpiration and plant growth and cannot be simply deduced from short-term mechanisms. Plant, Cell & Environment **40**, 846–857.

Tardieu F, Parent B, Caldeira CF, Welcker C. 2014. Genetic and physiological controls of growth under water deficit. Plant Physiology **164**, 1628–1635.

Tu Y, Jiang A, Gan L, *et al.* 2014. Genome duplication improves rice root resistance to salt stress. Rice **7**, 15.

Valkoun JJ. 2001. Wheat pre-breeding using wild progenitors. Euphytica **119**, 17–23.

Wang E, Engel T. 1998. Simulation of phenological development of wheat crops. Agricultural Systems **58**, 1–24.

Wang E, Martre P, Zhao Z, *et al*. 2017. The uncertainty of crop yield projections is reduced by improved temperature response functions. Nature Plants **3**, 17102.

Welcker C, Sadok W, Dignat G, Renault M, Salvi S, Charcosset A, Tardieu F. 2011. A common genetic determinism for sensitivities to soil water deficit and evaporative demand: meta-analysis of quantitative trait loci and introgression lines of maize. Plant Physiology **157**, 718–729.